

# NJC

Accepted Manuscript



This is an *Accepted Manuscript*, which has been through the Royal Society of Chemistry peer review process and has been accepted for publication.

*Accepted Manuscripts* are published online shortly after acceptance, before technical editing, formatting and proof reading. Using this free service, authors can make their results available to the community, in citable form, before we publish the edited article. We will replace this *Accepted Manuscript* with the edited and formatted *Advance Article* as soon as it is available.

You can find more information about *Accepted Manuscripts* in the [Information for Authors](#).

Please note that technical editing may introduce minor changes to the text and/or graphics, which may alter content. The journal's standard [Terms & Conditions](#) and the [Ethical guidelines](#) still apply. In no event shall the Royal Society of Chemistry be held responsible for any errors or omissions in this *Accepted Manuscript* or any consequences arising from the use of any information it contains.



[www.rsc.org/njc](http://www.rsc.org/njc)

## Self-propagating High-temperature Synthesis of aluminum substituted lanthanum ferrites $\text{LaFe}_{1-x}\text{Al}_x\text{O}_3$ ( $0 \leq x \leq 1.0$ )

Maxim V. Kuznetsov<sup>1\*</sup>, Iurii G. Morozov<sup>2</sup>, Ivan P. Parkin<sup>3</sup>

<sup>1</sup>All-Russian Research Institute on Problems of Civil Defense and Emergencies of Emergency Control Ministry of Russia (EMERCOM), Davidkovskaya Street 7, Moscow 121352 Russia  
[maxim1968@mail.ru](mailto:maxim1968@mail.ru)

<sup>2</sup>Institute of Structural Macrokinetics and Materials Science (ISMAN), Russian Academy of Sciences, Academician Osipyan Street 8, Chernogolovka, Moscow region, 142432 Russia  
[morozov@ism.ac.ru](mailto:morozov@ism.ac.ru)

<sup>3</sup>Materials Chemistry Research Centre, Department of Chemistry, University College London, 20 Gordon Street, London, WC1H 0AJ UK, [i.p.parkin@ucl.ac.uk](mailto:i.p.parkin@ucl.ac.uk)

Pure and aluminum substituted lanthanum ferrites  $\text{LaFe}_{1-x}\text{Al}_x\text{O}_3$  ( $x = 0-1.0$ ) were synthesized in air by self-propagating high-temperature synthesis (SHS) using iron or aluminum as sources of fuel. Two series of samples were produced: I – SHS in the absence of an external magnetic field (zero field SHS); II – SHS in a magnetic field of 0.27 T (applied field SHS); both series of samples were sintered at 1400<sup>0</sup> C for 65 h with intermediate grinding. Scanning electron microscopy, energy dispersive analysis of X-rays, X-ray powder diffraction and IR spectroscopy were carried out for both series of samples. XRD showed that for all the combustion products single phase orthorhombic ferrites were produced with a decrease in lattice parameters and unit cell volume with aluminum content (*e.g.*, for series I:  $x = 0$ ,  $V = 242.4 \text{ \AA}^3$ ;  $x = 1.0$ ,  $V = 217.3 \text{ \AA}^3$ ) as well as with magnetic field (*e.g.*, for series I:  $x = 0.3$ ,  $V = 233.8 \text{ \AA}^3$ ; for series II  $x = 0.3$ ,  $V = 232.8 \text{ \AA}^3$ ). <sup>57</sup>Fe Mössbauer indicated that at low Al concentrations ( $x \leq 0.3$ ) more than 92-93% of Fe atoms experience a perturbative disruption to their interatomic exchange interactions, consistent with the random distribution of  $\text{Al}^{3+}$  ions on the B sublattice. From  $x = 0.3$  Mössbauer spectra for both of the series showed the presence of a paramagnetic doublet together with a sextet, the percentage doublet component increased with  $x$  from 6.7% for  $x = 0.3$  to the 28.3% for  $x = 0.8$ . Room temperature magnetic measurements demonstrate weak ferromagnetism for all the iron-containing samples ( $x = 0-0.9$ ) with maximal magnetization in the range of 1.02-0.13 emu/g whereas  $\text{LaAlO}_3$  samples exhibit paramagnetic behavior. FT-IR spectra for both series I and II samples show predominantly two broad bands at 450-460 and 550-670  $\text{cm}^{-1}$ . Our experiments on weakly magnetic system  $\text{LaFe}_{1-x}\text{Al}_x\text{O}_3$  ( $0 \leq x \leq 1.0$ ) have provided evidence that

reorganisation of the green mixture along the field lines is one way in which the field acts. Reactions on powders and pellets have provided that evidence as well indicating that the magnetic field is important in determining the structural and magnetic characteristics of the product from a SHS reactions.

(\* Author to whom correspondence should be addressed)

## Introduction

Perovskite-type complex oxides ( $ABO_3$ ) have been widely used as elements of solid oxide fuel cells (SOFC) as well as high temperatures catalysts due to their thermal stability, well-definite structure and high electrical conductivity. Among them, orthorhombic  $LaFeO_3$  exhibits an unusual variety of magnetic properties and structural changes<sup>1-3</sup>. From the technological viewpoint, these compounds have been proposed for use as catalysts for CO oxidation and methane combustion<sup>4, 5</sup>. These materials are also known to be catalytically active for the complex oxidation of hydrocarbons and as combustion catalysts, as well as being used in gas sensors and solid-electrolytes<sup>6, 7</sup>. It was reported previously that the catalytic activity of Al-doped lanthanum orthoferrite were much higher than that of  $LaFeO_3$  due to the increase of high valence B-site cations and lattice oxygen content by the substitution of B-site elements<sup>2, 8</sup>.  $LaFeO_3$  is a suitable SOFC cathode due to its low reactivity with YSZ electrolyte in comparison to  $LaMnO_3$  at high temperatures<sup>9</sup>.

Rare-earth ferrites contain only trivalent metals in the structure, making them attractive systems for investigations of isovalent substitutions. From the magnetic viewpoint, it is also interesting to follow the structural, optical, electrical, magnetic and other properties transformation in this type of materials with partial and full substitution of ferromagnetic atoms ( $Fe^{3+}$ ) by paramagnetic ( $Al^{3+}$ ) ones<sup>10-15</sup>.  $LaFeO_3$  has an orthorhombic perovskite-like structure at room temperature<sup>16, 17</sup>. *Geller and Wood*<sup>16</sup> have reported that at high temperatures, X-ray diffraction indicates a phase transformation from the orthorhombic to the rhombohedral structure, but up to 845<sup>0</sup>C no phase transition is observed. At room temperature,  $LaAlO_3$  has a rhombohedral structure, which transforms to cubic at around 500<sup>0</sup>C<sup>16, 18, 19</sup>. The same transformation (orthorhombic-rhombohedral) were observed at  $x = 0.3$  by *Kuscer et al.*<sup>1</sup> for the samples prepared using standard ceramic technology whereas *Ciambelli et al.*<sup>8</sup> report all the  $LaFe_{1-x}Al_xO_3$  compounds in a range of 0-1.0 are orthorhombic. *Janbutrach et al.*<sup>14</sup> observed that  $LaFe_{1-x}Al_xO_3$  nanopowders prepared by polymerization complex method show the formation of the orthorhombic phase but with the second phase of  $\alpha-Fe_2O_3$ . *Brach et al.*<sup>20</sup> also successfully

studied  $^{139}\text{La}$  and  $^{27}\text{Al}$  NMR quadrupole effects in single crystals of the solid solution of  $\text{LaFe}_{1-x}\text{Al}_x\text{O}_3$ .

Traditional synthesis routes to aluminum substituted lanthanum ferrites involve two or multi steps procedures: firstly the heating of pelletized lanthanum hydroxide, iron and aluminum (III) oxides in air at  $1000^\circ\text{C}$ ; followed by sintering of the re-ground pellets in air at  $1200\text{--}1300^\circ\text{C}$  for up to  $100\text{ h}^{1, 4, 6}$ . Another method is via sol-gel involving citric acid as a complexing agent. The molar ratio of the metal ion to citrate was 1:2, and the preparation temperature of the gel was  $60\text{--}70^\circ\text{C}$ . The gel was dried at  $120^\circ\text{C}$  and annealed at  $650^\circ\text{C}$  for  $4\text{ h}^3$ . In the other method, a concentrated solution of the metal nitrates was mixed with an aqueous solution of citric acid by fixing at unity the molar ratio of citric acid to the metal cations. Water was evaporated from the mixed solution until a viscous gel was obtained. The gel was kept at  $80^\circ\text{C}$  overnight, ground and finally calcined at  $800^\circ\text{C}$  for  $5\text{ h}^8$ .

Here, we present a new method of synthesizing aluminum-substituted lanthanum ferrites by using self-propagating high-temperature synthesis (SHS) $^{21\text{--}24}$ . SHS is a fast exothermic reaction that produces easily sinterable near-to-final products in seconds by promotion of a synthesis wave through the material. Passage of the synthesis wave is driven by the exothermicity of the metals oxidation chemical reaction. Usually, SHS synthesis provides, after an annealing stage, a straightforward method of producing stoichiometric pure and substituted ferrite materials. When conducted in an applied magnetic field, the reaction produced a more homogeneous product than did the corresponding process from zero field synthesis. In most of the cases SHS products have high purity in comparison to the conventionally prepared ones due to the self-purification effect of the reacting components at high temperatures. During the SHS of ferrites, the magnetic starting components such as Fe and  $\text{Fe}_2\text{O}_3$  are partially aligned by the magnetic field, and this allows a more complete reaction to proceed.

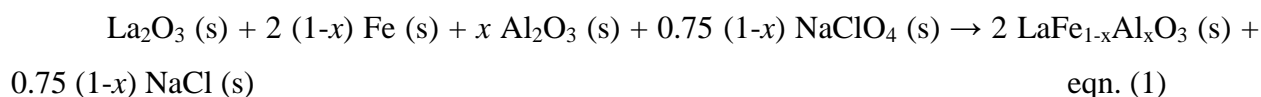
External magnetic fields can modify structural and combustion parameters of the systems containing ferromagnetic components. The rearrangement of powders in the initial blend and the nature of chemically ionized particles arising during the course of the combustion process determine the efficiency of action of the applied fields. The different SHS ferrites were prepared both in zero fields and in an applied field, and significant differences were observed in their post-sintering bulk structural and magnetic properties $^{25\text{--}27}$ . This result might prove to be a useful alternative to conventional modification methods.

## Experimental

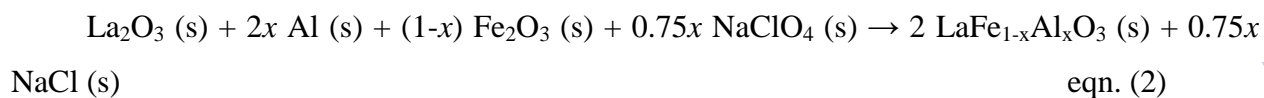
All reagents were obtained from Aldrich Chemical Company and used as supplied. Sodium perchlorate ( $\text{NaClO}_4$ ) was not assayed for particle size. Powders were weighed and mixed together under a nitrogen atmosphere inside a Saffron Scientific glove box. Nitrogen atmosphere was used because Fe and Al oxidize over a long period in air. A pestle and mortar was used to grind the reagents together. The green mixtures were made on a scale of few grams. The term “green mixture” describes the mixture of powder reagents on which SHS is performed. The SHS reaction is driven by exothermic oxidation of iron or aluminum metal. Sodium perchlorate was used as an internal oxidizing agent in the reaction. Lanthanum, iron or aluminum (III) oxides acts as a heat sink. This starting material (~1-2 g) was pressed isostatically with a pressure of 1 t into pellets with diameter of 13 mm and thickness of 2 mm or used in the form of powder (~10 g). The first kind of zero field SHS experiments were also carried out in air with pre-grounded powders in a ceramic boat. The same kind of applied field experiments were carried out using a ceramic boat containing powdered green mixture, which was placed between the “+” and “-” poles (N and S) of the permanent U-shape magnet providing a field of 0.27 T. A REKROW RK-2060 Micro Torch (UK) was used to ignite the powders or pellets from the lateral surface. SHS promoted an orange-yellow propagation wave, which traveled at  $U_{comb} = 3\text{-}5 \text{ mm s}^{-1}$  and  $T_{comb} = 1130\text{-}1330 \text{ }^\circ\text{C}$ . Reactions were analyzed *in situ* by optical pyrometry and slow motion video capture. Reaction products were obtained in essentially quantitative yields. They were ground and triturated with water to remove the traces of sodium chloride. Each intermediate SHS product was annealed at  $1400^\circ\text{C}$  for 65 h in a Nabertherm furnace with heating and cooling rates at  $10^\circ\text{C}/\text{min}$  to complete the reaction. All the final powder products were then analyzed by X-ray powder diffraction (Siemens D5000 diffractometer using filtered  $\text{CuK}\alpha$  radiation in the reflection mode with the consequent analysis performed using the ICDD PDF 4 database and Highcore software), vibrating sample magnetometry (performed on an EG&G Princeton Applied Research M4500 magnetometer at room temperature in applied fields of up to 13 kOe) and scanning electron microscopy/energy dispersive analysis by X-rays (SEM/EDAX using a Hitachi S4000). FT-IR- spectra were obtained on a Nicolet 205 using pressed KBr discs kept to a minimum (typically less than 1g of total reagents). All the  $^{57}\text{Fe}$  Mossbauer spectra were collected at room temperature on a Wissel MA-260S constant acceleration spectrometer, calibrated against  $\alpha$ -iron at room temperature. A triangular drive waveform was used, and the spectra were folded to remove baseline curvature. The spectra were least-squares fitted as a superposition of Lorentzian sextets and doublets.

### Sample preparation

SHS reactions were performed on the various starting mixtures of  $\text{La}_2\text{O}_3$ ,  $\text{Fe}_2\text{O}_3$ , Fe, Al,  $\text{Al}_2\text{O}_3$  and  $\text{NaClO}_4$ . The molar ratio of each reagent was chosen to confirm to the stoichiometry and oxygen content of the final product. Sodium perchlorate was used as an internal oxidizing agent for the combustion process. On decomposition, perchlorate produces oxygen, which oxidizes the Fe and Al metal fuel sources for the reaction. Sodium chloride is also produced on decomposition of the perchlorate. This provides additional energy for the reaction and acts as a wetting agent that helps to ensure passage of the propagation wave through the solid. The sodium chloride co-product is readily removed during the SHS itself (more than 70% of NaCl is sublimated according to Gay-Lussac's law) and the remaining traces of it were washed away with water. Different solid-state reagent mixtures were used across the both of  $\text{LaFe}_{1-x}\text{Al}_x\text{O}_3$  series. For the reaction with  $x \leq 0.4$ , Fe was used as a source of fuel and  $\text{Al}_2\text{O}_3$  as a source of Al:



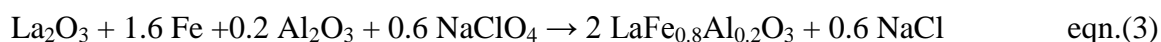
For higher levels of Al substitution ( $x > 0.5$ ), Al was used as a source of fuel and  $\text{Fe}_2\text{O}_3$  as a source of Fe:



All reactions were carried out in air. The limiting stage of the reactions is the oxidation state of the metal powders. Two different series of samples were prepared: series I – zero field SHS followed by a sintering at  $1400^\circ\text{C}$  for 65 h with intermediate grinding; and series II – SHS in an applied magnetic field of 0.27 T followed by a sintering at  $1400^\circ\text{C}$  for 65 h with intermediate grinding. In both of the series is underlined, the sintering was stopped after 25 h, the sample cooled to room temperature and reground, and sintering resumed for the remaining 40 h.

### Results and Discussion

Self-propagating high-temperature synthesis reactions were performed using various starting mixtures of  $\text{La}_2\text{O}_3$ ,  $\text{Fe}_2\text{O}_3$ , Fe,  $\text{Al}_2\text{O}_3$ , Al and  $\text{NaClO}_4$ . The molar ratio of each reagent was chosen to conform with the desired stoichiometry in the product. The reaction is driven by the exothermic oxidation of Fe or Al metal by oxygen, which was evolved from the sodium perchlorate decomposition. The perchlorate fully decomposed to oxygen and salt (NaCl) at  $600^\circ\text{C}$ . In the case  $\text{LaFe}_{0.8}\text{Al}_{0.2}\text{O}_3$  ( $x = 0.2$ ) the reaction scheme is shown in eqn. (3):



It should be noted that all the reactions were carried out in air using only solid oxidizers. The co-produced sodium chloride melts during the reaction and acts as an internal wetting agent allowing inter-diffusion of the reactants. Notably it is readily removed after the reaction by trituration of the product with water. The SHS preparation of pure and aluminium-substituted lanthanum orthoferrites is much quicker than standard conventional methods. Using SHS instead of the first annealing stage in the conventional synthesis reduces the reaction time from a few hours ca. 10 s. Two series of samples were prepared: SHS followed by a sintering at 1400<sup>0</sup> C for 65 h with intermediate grinding; and series II – SHS in an applied magnetic field of 0.27 T followed by a sintering at 1400<sup>0</sup> C for 65 h with intermediate grinding.

The combustion wave proceeded from the ignition point by means of yellow and yellow-red color, corresponding to a temperature of *c.a.* 1150-1250<sup>0</sup>C with propagation velocity of 3-4 mm/s. The reaction was driven by the oxidation of iron and aluminum metals. The sodium perchlorate acts as an inner oxidizing agent, providing further reaction energy after its decomposition and some sodium chloride that acts as a wetting agent in the process to help the diffusion of ions at the reaction front. Lanthanum, iron and aluminum (III) oxides provide a source of an appropriate metals for the final product and act as a moderators absorbing some of the reaction enthalpy. The combustion limit for the LaFe<sub>1-x</sub>Al<sub>x</sub>O<sub>3</sub> compounds was *x* = 0.5 in terms of using Fe metal as the fuel. By using the physical action of the magnetic field together with the chemical one (substitution), it was found possible to make a significant influence on the combustion characteristics such as maximum temperature and propagation velocity. It was also found that the application of the magnetic field affected the structural and magnetic characteristics of the synthesized material even after sintering at 1400<sup>0</sup>C. For all of the reactions, the measured reaction temperature exceeds the Curie temperatures of the ferromagnetic or ferrimagnetic reactants and products. However, the field may be acting by other mechanisms above the Curie temperature; for example, it may act on ions in molten phases in the reaction zone. An applied magnetic field leads to a greater degree of conversion of the reactants to the products. The better degree of conversion in the applied field product is related to the higher temperatures reached in the reaction, *ca.* 1200-1250 °C in applied field compared with 1150-1200 °C in zero field.

**XRD measurements.** The synthesis conditions also affect the unit cell volume of the products. At the room temperature LaFe<sub>1-x</sub>Al<sub>x</sub>O<sub>3</sub> solid solutions have an orthorhombic perovskite

structures. The X-ray diffraction patterns agreed with literature measurements for conventionally prepared materials<sup>8</sup>. The Al<sup>3+</sup> ions are incorporated on the Fe sites due to the relatively similar ionic radii  $r(\text{Fe}^{3+}) = 0.0645 \text{ nm}$ ,  $r(\text{Al}^{3+}) = 0.0535 \text{ nm}$ . Substitution of iron by aluminum in LaFe<sub>1-x</sub>Al<sub>x</sub>O<sub>3</sub> decreases the average size of ions in the B sites of ABO<sub>3</sub> perovskite structure, which leads to a reduction of the unit cell volume. The unit cell volume decreases linearly with  $x$  due to the smaller ionic radii of Al<sup>3+</sup> in accordance with the Vegard law. The lattice parameters  $a$ ,  $b$  and  $c$  as well as cell volumes  $V$  showed a quasi-linear decrease with Al content ( $x$ ) as well as for the use of an applied magnetic field for the same chemical composition (effect of “compression” of the lattice parameters under conditions of an applied field). There are small difference in the overall percentage decrease in cell size for series I and II. Since these materials are sintered well above their Curie temperatures, it may be attributed to the effect of the applied magnetic field in the initial synthesis stage, but not to a magnetostriction effect. Notably, the unit cell volume and other parameters decreased with aluminum content and with the application of an external magnetic field during SHS, as indicated in Table 1. Representative X-ray diffractograms are shown in Fig.1.

**SEM and BET characterization.** SEM/EDAX and electron probe measurements of both series of sintered samples showed that the materials were homogeneous with the expected La:Fe:Al elemental ratios. SEM showed micron sized agglomerates of crystallites (Fig.2). Particle sizes and surface areas are in the range of 40-82 nm and 1.1-3.0 m<sup>2</sup>/g respectively. The specific surface area of pure SHS lanthanum ferrite is 3.0 m<sup>2</sup>/g, which is higher than the aluminum doped materials (1.1-2.2 m<sup>2</sup>/g).

**Magnetic measurements.** LaFeO<sub>3</sub> and the samples with high iron content were found to be weakly ferromagnetic, whereas at high aluminum content (1.0), the samples exhibit paramagnetic behavior, which is an agreement with previously reported results<sup>28,29</sup>. All the iron-containing samples demonstrate weak ferromagnetism with maximal magnetization ( $\sigma_{\text{max}}$ ) in the range of 1.0-0.13 emu/g for  $x = 0-0.9$  (Fig.3). The maximum and remanent magnetization are higher for the products produced for the pelletized samples in comparison to the powdered ones for the same chemical compositions. At the same time, the value of magnetization is also higher for products obtained in applied magnetic field (0.27 T) in comparison for zero field ones. For example, for the LaFeO<sub>3</sub> (pellet) sample  $\sigma_{\text{max}} = 1.02 \text{ emu/g}$  after combustion in an applied field whereas at the same synthesis conditions  $\sigma_{\text{max}}$  of powdered LaFeO<sub>3</sub> sample is equal to 0.93 emu/g. The weak ferromagnetism in the  $x = 0$  samples arises from spin-canting induced by the Dzyaloshinsky interaction<sup>30</sup> and is apparent in the small magnetization ( $\sigma_{\text{max}} \sim 1.0 \text{ emu/g}$  in series I). Adding a small amount of Al disrupts the Fe-Fe exchange interactions, leading to



reduced atomic moments and a reduced magnetization. Increasing of the Al content breaks up the exchange interactions and leads to the formation of inhomogeneous disruption and paramagnetic states at the highest Al concentration ( $x = 1.0$ ). Using sodium perchlorate as an internal source of oxygen gives similar effects as a magnetic field, whether the reactions are performed in or out of a field, and on powders or pellets. Therefore, the unique effects of the field are a fibrous macrostructure and possibly a different reaction route. The magnetisation and coercive field of pure and aluminum doped lanthanum ferrite are modified by synthesis in a magnetic field and by using an internal oxidizing agent such as sodium perchlorate. The annealed product was found to have a reduced coercive field compared to the zero field one. The reduction in coercive field of the annealed products is attributed to better combustion, which leads to fewer pinning centres in the post-SHS / annealed product. Pinning centres are generally defects in the crystalline structure, or at grain boundaries. Fewer pinning centres means less resistance to domain wall motion, and consequently a lower coercivity. The influence of the field remained even after annealing; the annealed  $\text{LaFe}_{1-x}\text{Al}_x\text{O}_3$  products showed in some cases up to four times greater reduction in coercive force when made in a magnetic field.

**Optical measurements.** FT-IR spectra for both series I and series II samples show predominantly double broad bands at 450-460 and 550-670  $\text{cm}^{-1}$ . The second band shifts almost linearly from 550  $\text{cm}^{-1}$  for  $\text{LaFeO}_3$  to 670  $\text{cm}^{-1}$  for  $\text{LaAlO}_3$ .

It may be explained in terms of the modification of the exchange interaction between the Fe atoms with isovalent substitution of iron by smaller aluminum atoms. With increased  $x$  the  $\nu_{\text{Fe-O}}$  shifts occurring due to deformation in the structure of Fe-O polyhedrons. SEM/EDAX and electron probe measurements of both series of sintered samples showed that the materials were homogeneous with the expected La:Fe:Al elemental ratios. SEM showed micron sized agglomerates of crystallites.

*Changing colour of the intermediate SHS-products (without supplementary sintering) in the  $\text{LaFe}_{1-x}\text{Al}_x\text{O}_3$  system with increasing degree of Fe to Al substitution ( $x$ ).*

Changes in colour (observed earlier by Liu *et al.*<sup>15</sup>) of the intermediate synthesis products (SHS products without sintering) occur can be associated with two “sub-systems” of  $\text{LaFe}_{1-x}\text{Al}_x\text{O}_3$  solid solutions with  $x$  ranges of 0 - 0.4 and 0.6 - 1.0. It was impossible to initiate the combustion reaction in the system with  $x = 0.5$  by using only Al as well as only Fe metal powders as a source of fuel. This was connected with low degree of fuel from the calculated stoichiometric mixtures. Combined fuel (Fe+Al) use is not an attractive solution due to risk of undesirable compounds (Fe-Al intermetallides) formation at the temperatures of SHS- process.

Colour changes in the final product of the system with  $x = 0 - 0.4$  (Fuel - Fe metal powder) took place from brown (for  $x = 0$ ) to beige (for  $x = 0.4$ ) and was strongly connected with an increasing of amount of white-colour  $\text{Al}_2\text{O}_3$  which was used as a source of Al in the lanthanum-aluminum orthoferrite. It also seems to be connected with a reduction of the propagation rate with increasing  $x$ . With greater substitution ( $x$ ), the Fe fuel percentage was reduced from 25.5% mass. (at  $x = 0$ ) to 15.5% mass. (at  $x = 0.4$ ).

Colour changes in the system with  $x = 0.6 - 1.0$  (Fuel - Al metal powder) took place from the dark-brown (for  $x = 0.6$ ) to light gray (for  $x = 1.0$ ). The dark-brown color at  $x = 0.6$  was connected with using  $\text{Fe}_2\text{O}_3$  oxide as a source of Fe in the system studied. Its quantity at  $x = 0.6$  was 15.1% by mass. With high  $x$  quantity of  $\text{Fe}_2\text{O}_3$  was reduced and at  $x = 1.0$ , when whole iron was substituted by aluminum, the combustion product was light grey. The Al metal powder quantity at the same time increased from 7.7% mass. (for  $x = 0.6$ ) up to 14.2% mass. (for  $x = 1.0$ ). The possibility of a combustion process initiation at low quantity of the Al-fuel was related to its rather high chemical activity comparably to the Fe-fuel.

**Mössbauer measurements.** Mössbauer spectra for pure and Al doped samples are presented in Fig.4. This was measured at room temperature for the following samples of both series:  $\text{LaFeO}_3$ ,  $\text{LaFe}_{0.7}\text{Al}_{0.3}\text{O}_3$  and  $\text{LaFe}_{0.2}\text{Al}_{0.8}\text{O}_3$ . The spectra of the pure  $\text{LaFeO}_3$  samples showed a single Fe (III) sextet component with sharp lines, confirming that all the iron atoms are in equivalent crystallographic positions. On the introduction of Al into the lattice (i) a second subcomponent spectrum, a doublet, appears, and (ii) the sextet lines become broader. These features correspond to (i) an increasing fraction of the  $\text{Fe}^{3+}$  ions encountering severe disruption to their interatomic magnetic exchange interactions, leading to their adopting a paramagnetic state; and (ii) the remaining  $\text{Fe}^{3+}$  ions encountering an increasing degree of perturbative disruption to their local environments, leading to the reduction of the mean hyperfine fields. The measured reduction in hyperfine field varies smoothly and linearly with Al content. The parameters obtained from the fitting of the theoretical curve to the experimental spectra are presented in Table 2. It consists of a single magnetically ordered site for  $x = 0$  with isomer shift and quadrupole splitting values being typical for  $\text{Fe}^{3+}$ . The spectra of low levels of substitution agrees very well with that previously reported<sup>1, 23, 24</sup>. For  $x = 0$ , only one sextet was required to fit the experimental curve whereas for the  $x = 0.3$ , it comes from two magnetically ordered subspectra, and for the  $x = 0.8$  – three subspectra, with isomer shift and quadrupole splitting values characteristics of  $\text{Fe}^{3+}$ . It indicates that addition of Al does not change the valence state of the iron ions and all the iron ions in  $x = 0$ ; 0.3 and 0.8 samples are in the  $3^+$  valence and there are no anion vacancies. The data show that in both series of samples, the incorporation of increasing amounts of Al into the

orthoferrite lattice results in the growth of a paramagnetic doublet component and, the accompanying reduction in the mean hyperfine field and an increased broadening of a magnetic sextet component. For the  $x = 0.3$  samples the doublet area is on order 6-7%, indicating that the aluminum substitution is largely homogeneous with up to 93-94% of the Fe atoms experiencing only perturbative disruption to their exchange interactions that would be expected for a random substitution of Al. At higher Al concentrations, the paramagnetic doublet becomes associated with the Fe lattice as a whole. The doublet area in the  $x = 0.8$  samples is of the order 27-28%. Differences between the two series are minor and relate primarily to the relative areas of doublet and sextet components as well as the mean hyperfine fields of sextet components (see Table 2). None of the sintered samples has shown any signs of unreacted reagents. The Mössbauer spectra of the sintered products are very similar, seemingly independent of whether the reaction was conducted in a magnetic field.

## Conclusion

We have shown that a full range of single-phase pure and aluminum-substituted lanthanum orthoferrites  $\text{LaFe}_{1-x}\text{Al}_x\text{O}_3$  ( $0 \leq x \leq 1.0$ ) can be synthesized in air via SHS in which a combustion reaction is initiated between lanthanum (III) oxide, iron (III) oxide, aluminum (III) oxide and iron (or aluminum) metal powders followed by sintering at  $1400^\circ\text{C}$  for 65 h with intermediate grinding. The parameters of combustion wave were follows: temperature of *c.a.*  $1150\text{-}1250^\circ\text{C}$  and propagation velocity of 3-4 mm/s. It was shown, that there is a correlation between the temperature reached in the SHS reaction, the microstructure of the products and reaction completeness of the post-SHS product and the magnetic parameters of the annealed product. Higher reaction temperatures appear to be responsible for the greater degree of conversion of the reactants and the reduction in coercive field of the annealed product. X-ray diffraction data showed a systematic decrease in lattice parameters ( $a$ ,  $b$  and  $c$ ) and unit cell volume with aluminum content ( $x$ ) (e.g. for series I and  $x = 0$ ;  $V = 242.4 \text{ \AA}^3$ ;  $x = 1.0$ ;  $V = 217.3 \text{ \AA}^3$ ) as well as zero or applied (0.27 T) magnetic field usage for the same  $x$  (e.g. for series I and  $x = 0.2$ ;  $V = 238.0 \text{ \AA}^3$ , whereas for series II and  $x = 0.2$ ;  $V = 234.8 \text{ \AA}^3$ ). All the samples with high iron content values were found to be weakly ferromagnetic (with maximum magnetization ( $\sigma_{\text{max}}$ ) in the range of 0.99-0.13 emu/g for  $x = 0\text{-}0.9$ ), whereas at high aluminum content (1.0) the samples exhibit paramagnetic behavior.  $^{57}\text{Fe}$  Mössbauer spectroscopy indicated that at low Al concentrations (up to 0.3) more than 92-93% of the Fe atoms experiences a perturbative disruption to their interatomic exchange interactions, consistent with the random distribution of  $\text{Al}^{3+}$  atoms on the B sublattice. The remaining 7-8% of Fe atoms was observed in a paramagnetic state, indicating that

a small degree of inhomogeneous Fe clustering in the lattice. From  $x = 0.3$  the Mössbauer spectra for both of the series showed the presence of a paramagnetic doublet together with a sextet and that the percentage of doublet increase with  $x$  from 6.7% for  $x = 0.3$  to the 28.3% for  $x = 0.8$ . Mössbauer spectra for the  $x \geq 0.8$  samples show a paramagnetic doublet.

### Acknowledgements

The authors thank the Royal Society for the UK-FSU Collaborative Linkage Grant that facilitated this work. Present work was partially supported by the Russian Foundation for Basic Researches (RFBR) grants 13-03-12407-(ofi\_m2) and 13-03-12412-(ofi\_m2). Prof. Quentin A. Pankhurst (UCL) collected the Mössbauer spectra under the auspices of the UCL Intercollege Research Service.

### References

1. D. Kuščer, D. Hanžel, J. Holc, M. Hrovat and D. Kolar, *Journal of the American Ceramic Society*, 2001, **84**, 1148-1154.
2. J. Hole, D. Kuščer, M. Hrovat, S. Bernik and D. Kolar, *Solid State Ionics*, 1997, **95**, 259-268.
3. Z. Zhong, K. Chen, Y. Ji and Q. Yan, *Applied Catalysis A: General*, 1997, **156**, 29-41.
4. D. Kuščer, M. Hrovat, J. Holc, S. Bernik and D. Kolar, *Journal of Materials Science Letters*, 1996, **15**, 902-904.
5. M. Hrovat, J. Holc, D. Kuscer, Z. Samardzija and S. Bernik, *Journal of Materials Science Letters*, 1995, **14**, 265-267.
6. D. Kuščer, J. Holc, M. Hrovat and D. Kolar, *Journal of the European Ceramic Society*, 2001, **21**, 1817-1820.
7. D. Kuščer, F. Dimc, J. Holc, M. Hrovat, S. Bernik and D. Kolar, *Journal of Materials Science Letters*, 1996, **15**, 974-976.
8. P. Ciambelli, S. Cimino, G. Lasorella, L. Lisi, S. De Rossi, M. Faticanti, G. Minelli and P. Porta, *Applied Catalysis B: Environmental*, 2002, **37**, 231-241.
9. H. Yokokawa, N. Sakai, T. Kawada and M. Dokiya, *Solid State Ionics*, 1992, **52**, 43-56.
10. S. Acharya and P. K. Chakrabarti, *Solid State Communications*, 2010, **150**, 1234-1237.
11. S. Acharya, A. K. Deb, D. Das and P. K. Chakrabarti, *Materials Letters*, 2011, **65**, 1280-1282.
12. M. A. Ahmed, N. Okasha and B. Hussein, *Journal of Magnetism and Magnetic Materials*, 2012, **324**, 2349-2354.
13. M. A. Ahmed, N. Okasha and B. Hussein, *Journal of Alloys and Compounds*, 2013, **553**, 308-315.
14. Y. Janbutrach, S. Hunpratub and E. Swatsitang, *Nanoscale Research Letters*, 2014, **9**, 498.
15. L. Liu, A. Han, M. Ye and M. Zhao, *Solar Energy Materials and Solar Cells*, 2015, **132**, 377-384.
16. S. Geller and E. A. Wood, *Acta Crystallographica*, 1956, **9**, 563-568.
17. T. Nakamura, G. Petzow and L. J. Gauckler, *Materials Research Bulletin*, 1979, **14**, 649-659.
18. S. Geller, *Acta Crystallographica*, 1957, **10**, 243-248.

19. G. W. Berkstresser, A. J. Valentino and C. D. Brandle, *Journal of Crystal Growth*, 1991, **109**, 457-466.
20. B. Y. Brach, S. P. Gabuda, A. M. Panich and R. M. Rakhmankulov, *Journal of Structural Chemistry*, 1984, **24**, 929-930.
21. T. Sathitwitayakul, M. V. Kuznetsov, I. P. Parkin and R. Binions, *Sensor Letters*, 2014, **12**, 1567-1571.
22. M. V. Kuznetsov, I. P. Parkin, D. J. Caruana and Y. G. Morozov, *Journal of Materials Chemistry*, 2004, **14**, 1377-1382.
23. M. V. Kuznetsov, Q. A. Pankhurst, I. P. Parkin and Y. G. Morozov, *Journal of Materials Chemistry*, 2001, **11**, 854-858.
24. W. B. Cross, L. Affleck, M. V. Kuznetsov, I. P. Parkin and Q. A. Pankhurst, *Journal of Materials Chemistry*, 1999, **9**, 2545-2552.
25. M. V. Kuznetsov, Q. A. Pankhurst, I. P. Parkin, L. Affleck and Y. G. Morozov, *Journal of Materials Chemistry*, 2000, **10**, 755-760.
26. L. Affleck, M. D. Aguas, I. P. Parkin, Q. A. Pankhurst and M. V. Kuznetsov, *Journal of Materials Chemistry*, 2000, **10**, 1925-1932.
27. M. V. Kuznetsov, S. M. Busurin, Y. G. Morozov and I. P. Parkin, *Physical Chemistry Chemical Physics*, 2003, **5**, 2291-2296.
28. J. C. Wood, *Bulletin of the American Physical Society*, 1968, **3**, 574.
29. N. A. Halasa, G. DePasquali and H. G. Drickamer, *Physical Review B*, 1974, **10**, 154-164.
30. I. Dzyaloshinsky, *Journal of Physics and Chemistry of Solids*, 1958, **4**, 241-255.

**Table 1.** Lattice parameters for two series of  $\text{LaFe}_{1-x}\text{Al}_x\text{O}_3$  orthoferrites obtained following the SHS reaction of Fe, Al,  $\text{Fe}_2\text{O}_3$ ,  $\text{La}_2\text{O}_3$ ,  $\text{Al}_2\text{O}_3$  and  $\text{NaClO}_4$  either in zero field (denoted I) or in an applied field of 0.27 T (denoted II). In both cases, sintering at  $1400^\circ\text{C}$  for 65 h with intermediate grinding followed the initial SHS preparation. The lattice parameters and unit cell volumes listed were obtained by X-ray analysis at room temperature.

$x$	$a/\text{\AA}$ , ( $\pm 0.004$ )	$b/\text{\AA}$ , ( $\pm 0.004$ )	$c/\text{\AA}$ , ( $\pm 0.004$ )	$V/\text{\AA}^3$ , ( $\pm 0.5$ )
0 (I)	5.560	5.551	7.854	242.4
0 (II)	5.550	5.543	7.843	241.3
0.1 (I)	5.552	5.527	7.839	240.8
0.1 (II)	5.548	5.518	7.834	239.8
0.2 (I)	5.550	5.490	7.811	238.0
0.2 (II)	5.491	5.481	7.803	234.8
0.3 (I)	5.485	5.473	7.788	233.8
0.3 (II)	5.477	5.464	7.779	232.8
0.4 (I)	5.441	5.427	7.743	228.6
0.4 (II)	5.422	5.413	7.761	227.8
0.6 (I)	5.374	5.372	7.703	222.4
0.6 (II)	5.370	5.369	7.699	222.0
0.7 (I)	5.370	5.369	7.694	221.9
0.7 (II)	5.368	5.366	7.681	221.2
0.8 (I)	5.368	5.364	7.651	220.3
0.8 (II)	5.364	5.361	7.643	219.8
0.9 (I)	5.363	5.360	7.622	219.1
0.9 (II)	5.360	5.354	7.618	218.6
1.0 (I)	5.357	5.351	7.579	217.3

**Table 2.** Room temperature Mossbauer parameters for  $\text{LaFe}_{1-x}\text{Al}_x\text{O}_3$  ferrites-aluminates produced by SHS in zero field (denoted I) and in an applied magnetic field 0.27 T (denoted II) followed by sintering at  $1400^\circ\text{C}$  for 65 h with intermediate grinding. The spectra were least-squares fitted as a superposition of Lorentzian sextets and doublets. The parameters listed are the isomer shift  $\delta$  ( $\pm 0.01$  mm/s), quadrupole splitting  $\Delta$  ( $\pm 0.01$  mm/s), quadrupole shift  $2\varepsilon$  ( $\pm 0.01$  mm/s) and hyperfine field  $B_{\text{hf}}$  ( $\pm 0.1$  T).

$x$	$\delta$ , mm/s	$\Delta$ mm/s	$2\varepsilon$ mm/s	$B_{\text{hf}}$ (kOe)
0 (I)	0.35(89)	0.14(25)	-0.05(89)	522
0 (II)	0.36(10)	0.14(30)	-0.05(10)	521
0.3 (I)	0.36(12)	0.14(32)	-0.05(12)	520
	0.30(37)	0.43(56)	-	-
0.3 (II)	0.36(93)	0.14(24)	-0.05(93)	520
	0.28(31)	0(85)	-	-
0.8 (I)	0.36(89)	0.15(20)	-0.07(88)	511
	0.39(72)	-	-0.04(70)	456
	0.32(12)	0.32(28)	-	-
0.8 (II)	0.36(40)	0.13(99)	-0.10(40)	512
	0.33(76)	-	-0.15(74)	464
	0.32(91)	0.28(36)	-	-

**Figure Caption**

**Figure 1.** X-ray powder diffraction patterns for: 1 -  $\text{LaFe}_{0.2}\text{Al}_{0.8}\text{O}_3$  obtained via SHS reaction undertaken in the presence of an external applied field of 0.27 T; 2 -  $\text{LaFe}_{0.7}\text{Al}_{0.3}\text{O}_3$  obtained via SHS in zero field; 3 -  $\text{LaFe}_{0.7}\text{Al}_{0.3}\text{O}_3$  obtained via SHS in a field of 0.27 T; 4 -  $\text{LaFeO}_3$  obtained via SHS in a field of 0.27 T. The peaks corresponding to the planes (hkl) for  $\text{LaFeO}_3$  (JCPDS 74-2203) are indexed. Asterisks denoted  $\text{La}(\text{OH})_3$  (JCPDS 06-0585) secondary phase. All data determined for sintered material ( $1400^\circ\text{C}$  for 65 h).

**Figure 2.** SEM micrographs of  $\text{LaFe}_{1-x}\text{Al}_x\text{O}_3$  samples derived from SHS reaction: (a)  $x = 0.0$  (series I, 5 kV, x1000); (b)  $x = 0.3$  (series II, 5kV, x10000).

**Figure 3.** Representative magnetization curves at room temperature for  $\text{LaFe}_{1-x}\text{Al}_x\text{O}_3$  samples derived from SHS reaction in an external magnetic field of 0.27 T (series II): 1 -  $\text{LaFeO}_3$ ; 2 -  $\text{LaFe}_{0.7}\text{Al}_{0.3}\text{O}_3$ ; 3 -  $\text{LaFe}_{0.4}\text{Al}_{0.6}\text{O}_3$ ; 4 -  $\text{LaFe}_{0.3}\text{Al}_{0.7}\text{O}_3$ ; 5 -  $\text{LaFe}_{0.1}\text{Al}_{0.9}\text{O}_3$ . All data determined for samples obtained after post-SHS sintering at  $1400^\circ\text{C}$  for 65 h.

**Figure 4.** Room temperature Mössbauer spectra for  $\text{LaFe}_{1-x}\text{Al}_x\text{O}_3$  ( $x = 0; 0.3; 0.8$ ) derived from SHS reaction in zero field and in an external magnetic field of 0.27 T. All the data are for samples obtained after post-SHS sintering at  $1400^\circ\text{C}$  for 65 h.



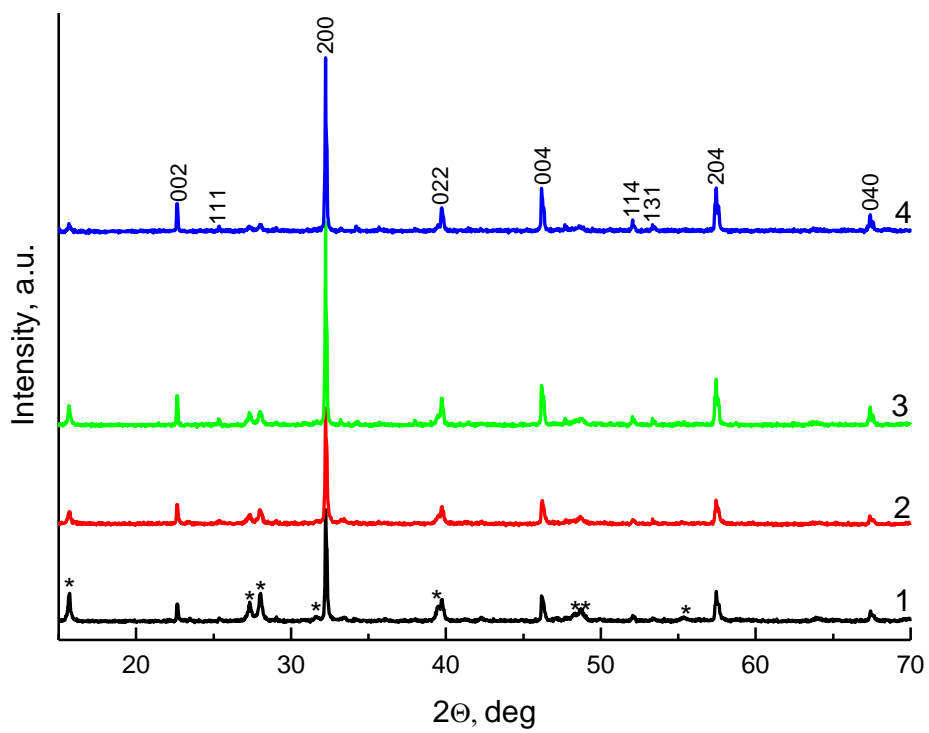
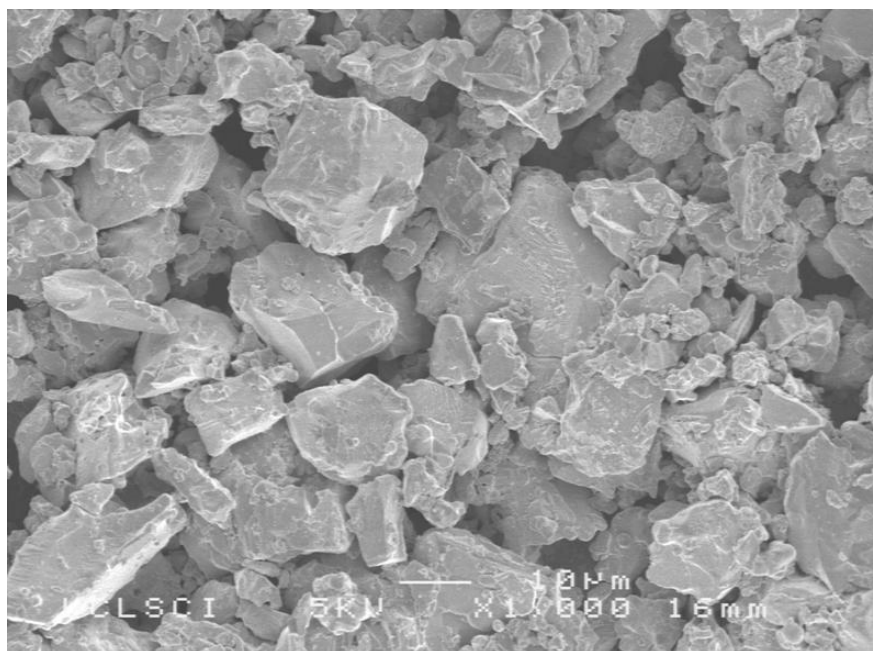
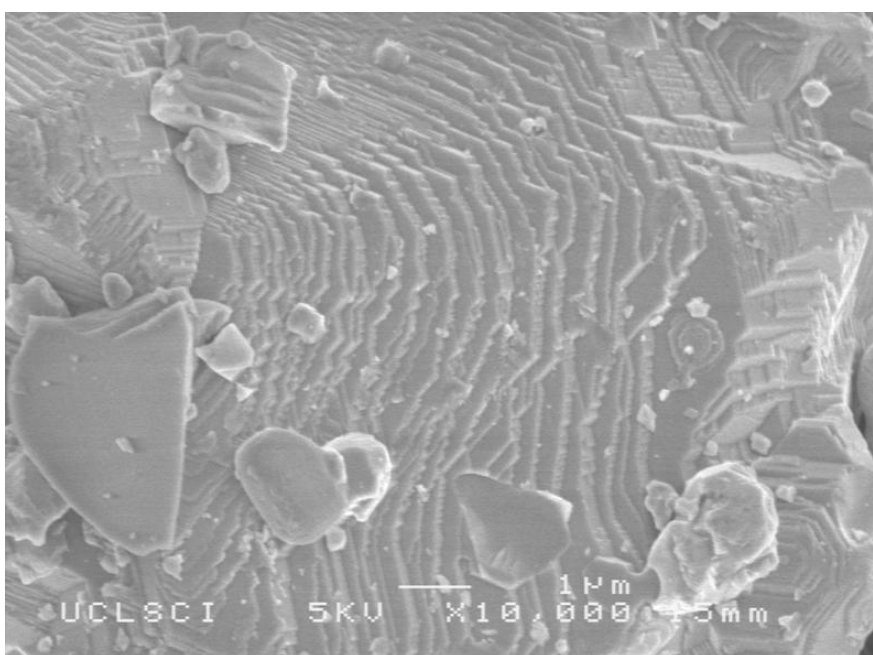


Figure 1



**Figure 2a**



**Figure 2b**

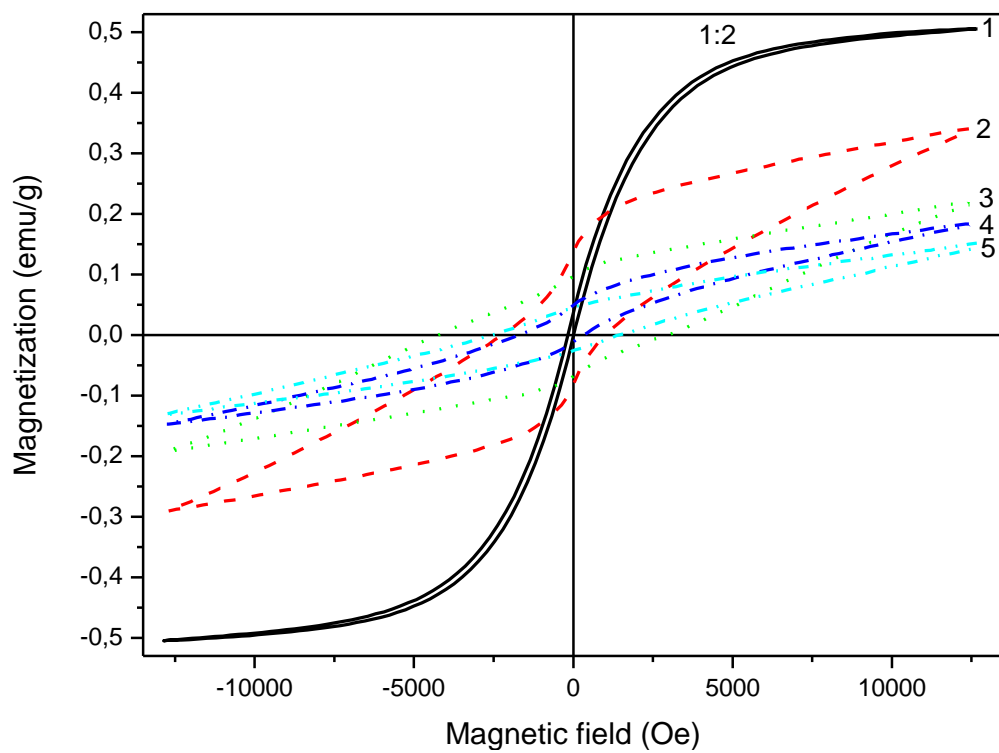


Figure 3

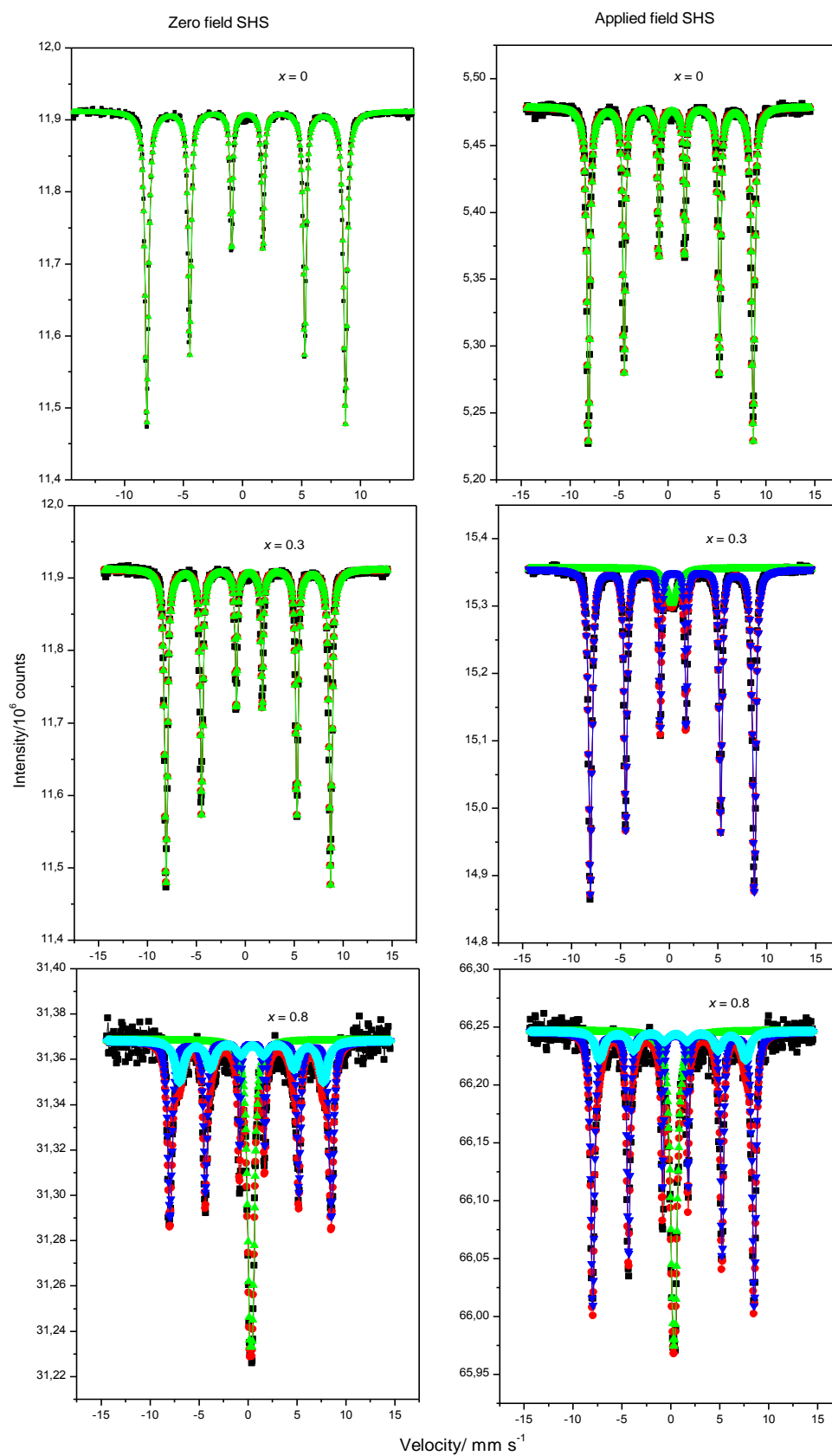
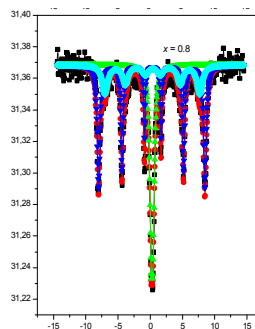


Figure 4



External magnetic field results in more complete combustion reaction as well as structural, magnetic and Mössbauer characteristics of ferrites changing